Robotics and Autonomous Systems 152 (2022) 104065

Contents lists available at ScienceDirect

Robotics and Autonomous Systems

journal homepage: www.elsevier.com/locate/robot

Safe and adaptive autonomous navigation under uncertainty based on sequential waypoints and reachability analysis

Nadhir Mansour Ben Lakhal [a,b,*], Lounis Adouane [c], Othman Nasri [b], Jaleleddine Ben Hadj Slama [b]

[a] Institut Pascal, UCA/SIGMA – UMR CNRS 6602, Clermont Auvergne University, 63178 Aubière cedex, France
[b] LATIS Lab, National Engineering School of Sousse (ENISo), University of Sousse, BP 264 Sousse Erriadh 1023, Tunisia
[c] CNRS, Heudiasyc, UMR 7253, Université de Technologie de Compiègne, 60203 Compiègne, France

ARTICLE INFO

Article history:
Received 28 May 2021
Received in revised form 28 January 2022
Accepted 8 February 2022
Available online 18 February 2022

Keywords:
Autonomous navigation
Sequential waypoint-based navigation
Risk assessment and management
Reachability analysis
Interval Taylor models

ABSTRACT

This paper presents a new approach for a safe autonomous navigation based on reliable state space reachability analysis. This latter improves an already proposed flexible Navigation Strategy based on Sequential Waypoint Reaching (NSbSWR) framework (Vilca et al., 2015), while considering explicitly different uncertainties in modeling and/or perception. Indeed, NSbSWR is an emergent concept that exploits its flexibility and genericity to avoid frequent complex trajectories' planning/re-planning. The paper's main contribution is to introduce a reachability analysis scheme as a reliable risk assessment and management policy ensuring safe autonomous navigation between the successive assigned waypoints. For this aim, interval analysis is employed to propagate uncertainties influencing the vehicle's dynamics into the navigation system states. By solving an ordinary differential equation with uncertain variables and parameters via an interval Taylor series expansion method, all the vehicle potential reachable state-space is revealed. According to the obtained bounds of the reachable sets, a decision about the navigation safety is made. Once a collision risk is captured, the risk management layer acts to update the control parameters to master the critical situation and guarantee a proper reaching of waypoint, while avoiding any risky state. Several simulation results prove the safety, efficiency and robustness of the overall navigation under uncertainties.

1. Introduction

During the last decades, great progresses have been witnessed in the field of intelligent transportation systems. Efforts have been spent to move towards more reliable and safe navigation approaches. Mobile robots as well autonomous vehicles navigation are generally based on accurate following of references trajectories. In this context, a multitude of sophisticated path planning and/or trajectory computation methods have been practiced [1–4]. Likewise, several control strategies have been introduced in the literature to track the reference trajectories [5,6]. However, within the technological advents brought by the community, new challenges have been recently raised for Autonomous Ground Vehicles (AGV) [7–9]. The ongoing attempts to improve AGV performances have led to complex and computationally demanding trajectory planners. More and more technical constraints must be then satisfied, which complicates the navigation task, mainly in highly dynamic and uncertain environment [10]. Modern AGVs are sensitive to localization and perception inaccuracy. Thus, following precisely a trajectory, while mastering unexpected risks in uncertain and dynamic navigation environments, is not always evident.

1.1. Navigation based on waypoints

Offering AGVs an important degree of freedom may be the key solution to face uncertainties and safety challenges. Allowing modern AGVs to act in several possible manners (choose another path, perform different maneuvers, etc.) can provide multiple backup solutions for critical situations. Accordingly, flexibility is now needed as never as a new requirement for AGVs. To address this issue, there is an increasing trend to substitute the conventional trajectory planners by waypoint assignment strategies [11–14]. Following particular points from a discretized path simplifies drastically the navigation mission. Instead of the arduous path following, few series of waypoints can be properly arranged to guide the vehicle. Contrarily to former approaches, AGVs move freely between the assigned waypoints until reaching a final desired destination.

* Corresponding author at: Institut Pascal, UCA/SIGMA – UMR CNRS 6602, Clermont Auvergne University, 63178 Aubière cedex, France.
E-mail address: Nadhir_Mansour.BEN_LAKHAL@etu.uca.fr (N.M. Ben Lakhal).

https://doi.org/10.1016/j.robot.2022.104065

Currently, the majority of the waypoint following-related work is almost focusing on optimizing this approach performances in terms of stability, traveling time and path smoothness [15,16]. Safety checking techniques dedicated to this sort of navigation have been roughly linked to obstacle avoidance [17]. Unquestionably, safety verification of the waypoint following approaches requires to be conducted from larger prospects. The appropriate reaching of waypoints under uncertainty is insufficiently investigated. Trajectory re-planning methods with the use of intermediate targets were used in [18]. An error feedback controller was employed to minimize waypoint tracking errors in [19]. Nevertheless, consistency of the adopted error model was not proven. With a posterior knowledge of the navigation environment, a view-matching vision-based approach was utilized to cross the selected waypoints in [20]. Differently in [21], the number and the size of waypoints were reconfigured via a genetic algorithm to reduce the path following errors. According to a Software verification concept, the authors in [22] developed a risk management that checks the temporal and logical behavior of the navigation. Needless to say, Software checking approaches may monitor a limited number of inputs, but cannot deal with the high uncertainty of the navigation dynamics [23].

The lack of safety guarantees for the waypoint-based navigation has profound impacts on its perspectives. Without these warranties, it remains restricted for environments without severe risks. Thanks to its advantages in performing a long-term horizon prediction, Reachability Analysis (RA)[1] has been recently exploited to solve several problems for AGVs, e.g., path parametrization, optimal control and risk identification [25,26].

1.2. Reachability analysis related work

The considerable available literature on RA has turned this research field into a very active one [24]. On the one hand, the system reachable sets may be revealed via different stochastic models. A particular Probability Distribution Function (PDF) can be selected to rule the transition probability of the system states i.e., the probability quantifying chances of moving from the system actual state to another one. For AGVs, the predicted states via stochastic approaches describes generally vehicles' future occupancy regions [27]. Then, the obtained states are exploited to proceed several tasks from the navigation process, such as localization, risk assessment, trajectories re-planing, etc. [27]. The polynomial chaos expansion and Markov processes are among the most widespread stochastic techniques used by the AGV community for the aforementioned purposes [28,29]. However, the reliability of the stochastic RA is still controversial. The definition of a PDF that fits the studied system requires huge amounts of historical data. Moreover, the stochastically derived reachable sets may mismatch reality due to potential changes in the system noise properties [30]. Furthermore, most of the stochastic RA approaches are sensitive to non-linearities of the navigation dynamics [31]. Therefore, huge efforts have been spent to increase these methods confidence. The work reported in [32] employed human-like driving models and empirical data to ameliorate the RA confidence-level to predict behaviors of other drivers and plan safe trajectories for AGVs. Focus has been given also for Monte Carlo multi-simulation to perform reachability for AGVs while assessing the in-road risks [27]. Simultaneous simulation executions of several driving maneuvers with distinct configurations are proceeded. According to the density of the results, occupancy regions of AGVs with the highest prediction probability are pointed out.

[1] RA refers to techniques that pre-estimate the future states of a dynamic system according to its initial states and its potential inputs/parameters [24].

As a cut off with the inaccurate stochastic RA, a new wave of set-membership methods have been emerged by relying on the geometrical extrapolation of the system states [33]. Data describing the system variables, inputs and parameters are enclosed into sets to consider the uncertainty e.g., ellipsoids, zonotopes, polytopes, etc. [34]. These sets are propagated through the system model to reveal its reachable space [35]. Using a complex set-representation of data may invoke a considerable computational cost. Although some enclosures are more compact than others (such as zonotopes and ellipsoids), proceeding the computation within these sets is complicated [36]. To simplify the computation through these sets, the studied system linearization is necessary, which entails severe modeling errors. In this regard, the authors in [23] used conservative abstraction methods to deal with the linearization errors impacting the RA performed for AGVs online safety verification.

Rather, extensive research works have been focused on the interval analysis, since intervals are easily handled by formal equations [37]. The reachable sets have been determined via branch and brought interval-based algorithms [38]. The results are accurate, but the recursive nature of these algorithms entails an unpredictable run-time. Another interval-based approaches count on the Differential Inequalities (DIs) that extract tight bounds of reachable sets for the monotonous systems [39]. Therefore, the DI application has been generalized by hybridizing systems into locally monotonous subsystems [40]. The interval Taylor expansion is another interval-based RA approach that may over-approximate a given system reachable states by solving an uncertain Ordinary Differential Equation (ODE) describing the studied system [41]. The system reachable sets are deduced easily by applying a set-integration within whole regions of initial states, inputs and parameters.

In the currently proposed paper, a RA scheme is developed for safety verification of an already proposed flexible Navigation Strategy based on a Sequential Waypoint Reaching (NSbSWR) [11,42]. All the AGV potential reachable state sets, while moving towards each currently assigned waypoint, are estimated via an interval-based Taylor series expansion. At the best of the authors' knowledge, this is the first proposed risk assessment and management strategy for the NSbSWR with guaranteed performances, since certain predictions are obtained through bounded computation to consider the perception and modeling uncertainties. Not only collision risks can be captured thanks to the proposed method, but also a feedback control solution is applied once a threat is identified. A collision-free reachable space for the AGV future states is obtained by acting on the control parameters.

The rest of this paper is organized as follows: Section 2 describes summarily the NSbSWR architecture and its different components. Section 3 details the proposed RA strategy and validates its consistency through extensive batch simulations. Section 4 presents also the proposed risk management policy based on the obtained RA results and proves its efficiency through simulations. Section 5 concludes this paper and discusses some future works.

2. Overall control architecture for NSbSWR

The target assignment strategy of the tackled NSbSRW was proposed initially in [42]. By allowing performing more maneuvers between waypoints thanks to the NSbSWR flexibility, it is no longer mandatory for AGVs to track precisely a given trajectory. The NSbSWR is also of a great genericity since the navigation turns to a trajectory tracking task when the distance between waypoints is kept short. The proposed work in this paper suggests a novel risk assessment and management level (cf. transparent yellow box in Fig. 1) of the studied NSbSWR under

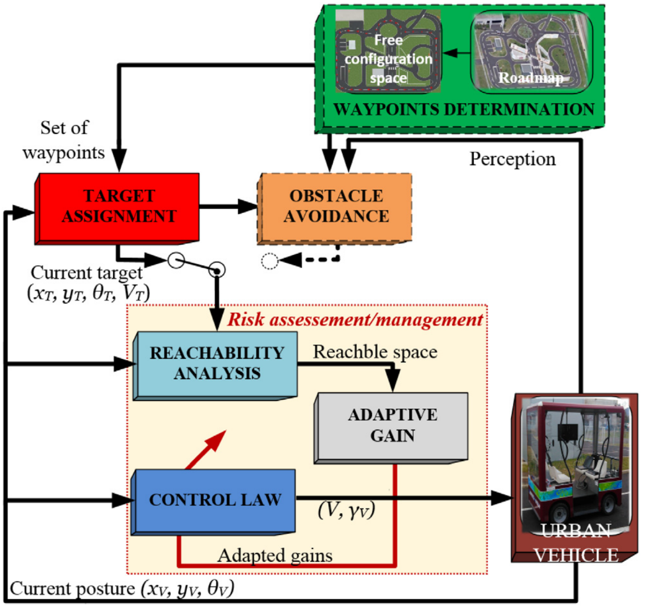

Fig. 1. NSbSWR control architecture. The part highlighted in yellow corresponds to the risk assessment and management blocks proposed in this paper. (For interpretation of the references to color in this figure legend, the reader is referred to the web version of this article.)

high uncertainties. Therefore, there is no intention to detail here the selection of the waypoint configurations i.e., each waypoint's position, orientation and velocity. A high level-planning task is devoted to accomplish this objective [11]. Accordingly, a general overview of the navigation based on waypoints (according to [11, 42]) is given below to understand the NSbSWR main components and to focus later on the principle contribution of this paper. In this sense, the overall control architecture dedicated to deal with such a navigation strategy is illustrated in Fig. 1. The main blocks of this architecture are listed below:

- The "Waypoint determination" block (dashed green box in Fig. 1) provides the set of appropriate waypoints configuration [11].
- The "Obstacle avoidance" block is activated when an obstacle obstructs the AGV's movement toward its target. The adopted obstacle avoidance method is based on limit-cycle technique which is detailed in [43].
- The "Control law" block guarantees an asymptotically stable reaching of waypoints (cf. Section 2.1).
- The "Target assignment" block selects at every sampling step the appropriate target to reach from the set of sequential waypoints (cf. Section 2.2).
- The "Reachability analysis" block is responsible of the risk assessment for the NSbSWR. It predicts any potential navigation risk while taking into account several modeling/perception uncertainties (cf. Section 2.3).
- The "Adaptive gain" block adapts the control law parameters (gains) to guarantee an appropriate management of risks already captured by the "Reachability analysis" block (cf. Section 2.3).

The different components composing the NSbSWR architecture are summarized in the sequel. The main propositions of the paper corresponding to the yellow part given in Fig. 1 will be detailed in Sections 3 and 4 respectively.

2.1. Control law

The waypoints are static targets located in the navigation space. Hence, any asymptotically stable controller can be used

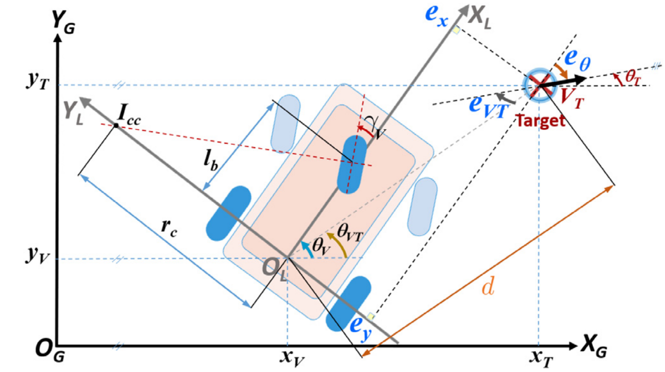

Fig. 2. Vehicle/target configurations and control variables.

for the NSbSWR. The control law adopted in this work showed interesting performances in different autonomous navigation applications, such as for safe ACC (Adaptive Cruise Control) in [44] and navigation formation in [45]. Let (x_V, y_V, θ_V) denote the vehicle posture at a global frame (O_G, X_G, Y_G). Then, a typical tricycle kinematic model is used to describe the vehicle motion:

$$\begin{cases} \dot{x}_V &= V\cos(\theta_V) \\ \dot{y}_V &= V\sin(\theta_V) \\ \dot{\theta}_V &= V\tan(\gamma_V)/l_b \end{cases} \quad (1)$$

where V is the vehicle linear velocity and γ_V is its front wheel orientation. V and γ_V are the two control inputs of the AGV (cf. Eqs. (5) and (6)). l_b indicates the vehicle's wheelbase. As can be seen from Fig. 2, I_{cc} is the center of curvature characterizing the vehicle's trajectory. The curvature and the radius of curvature, which are respectively noted c_c and r_c, obey to:

$$r_c = l_b/\tan(\gamma_V) \quad \text{and} \quad c_c = 1/r_c \quad (2)$$

The adopted controller is supposed to lead the AGV towards targets with non-holonomic constraints (cf. Fig. 2). Only the target pose (x_T, y_T, θ_T) and its velocity V_T are needed to perform the navigation. In fact, the control law is synthesized based on the following Lyapunov function V_L (cf. Fig. 2):

$$V_L = \frac{1}{2}\left(e_x^2 + e_y^2\right)[K_d + K_l \sin^2(e_{VT})] + K_o[1 - \cos(e_\theta)] \quad (3)$$

where $(e_x,\ e_y,\ e_\theta)$ are the navigation error states with regard to a local frame $(O_L,\ X_L,\ Y_L)$ (cf. Fig. 2). d and θ_{VT} indicate respectively the distance and the angle between the position of the vehicle and the target. $e_{VT} = \theta_T - \theta_{VT}$ is an error variable that identifies the vehicle position-related error while considering the target orientation θ_T. Note that the initial values of e_{VT} and e_θ must satisfy the following initial conditions:

$$e_{VT} \in\ ]-\pi/2, \pi/2[\quad \text{and} \quad e_\theta \in\ ]-\pi/2, \pi/2[\quad (4)$$

The desired linear velocity V and the front wheel orientation γ_V of the vehicle which permit to asymptotically stabilize the errors $(e_x, e_y, e_\theta, e_{VT})$ towards zero (allowing therefore to ensure $\dot{V}_L < 0$) are given by:

$$V = V_T\cos(e_\theta) + v_b \quad (5)$$

$$\gamma_V = \arctan(l_b c_c) \quad (6)$$

Afterwards, Eqs. (7) and (8) define v_b and c_c through a set of fixed gains $\mathbf{K} = (K_d, K_l, K_o, K_x, K_{VT}, K_\theta)$:

$$v_b = K_x[K_d e_x + K_l d\sin(e_{VT})\sin(e_\theta) + K_o\sin(e_\theta)c_c] \quad (7)$$

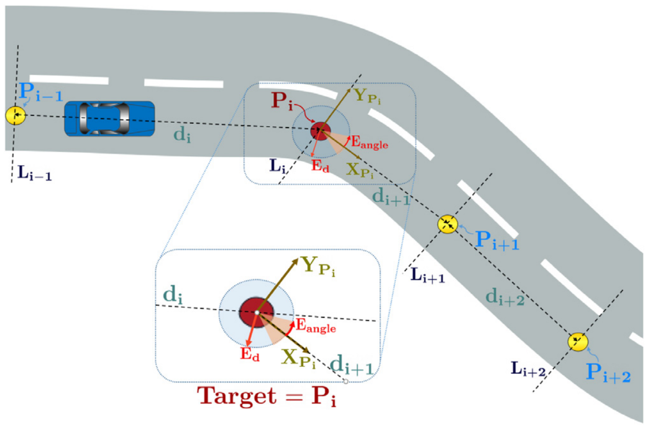

Fig. 3. Description of NSbSWR target assignment strategy [42].

$$c_c = \frac{1}{r_{c_T}\cos(e_\theta)} + \frac{d^2 K_l \sin(e_{VT})\cos(e_{VT})}{r_{c_T} K_o \sin(e_\theta)\cos(e_\theta)} + K_\theta \tan(e_\theta) + \frac{K_d e_y - K_l d \sin(e_{VT})\cos(e_\theta)}{K_o\cos(e_\theta)} + \frac{K_{VT}\sin^2(e_{VT})}{\sin(e_\theta)\cos(e_\theta)} \quad (8)$$

2.2. Sequential target assignment

The strategy to assign, at each sample time, the waypoint to reach by the vehicle is given in Algorithm 1. At every sample time, the relative pose between the vehicle and the target is checked. Then, a decision about whether to keep moving ahead the current target or to shift towards the next waypoint is made. Henceforward, the currently followed waypoint is called target. Let us consider a set of waypoints (cf. Fig. 3). Every pair of successive waypoints P_{i-1} and P_i are separated by a distance denoted d_i. The orientation of P_i, denoted θ_{P_i}, is given by [42]:

$$\theta_{P_i} = \arctan\left(\frac{y_{P_{i+1}} - y_{P_i}}{x_{P_{i+1}} - x_{P_i}}\right) \quad (9)$$

The error conditions, E_d and E_{angle}, are used to switch to the next waypoint when the vehicle's position is inside a circle given by the center (x_{P_i}, y_{P_i}) and a radius E_d. Hence, the current waypoint index is updated with the next waypoint and the vehicle has to adapt its movement according to this new target.

Owing to control imperfections, it is not always possible to lead accurately the vehicle towards the error circle. In such a critical situation, a backup countermeasure must be tackled to carry on the navigation and ensure its liveness. In that case, the local target frame $X_{P_i}Y_{P_i}$ is used. The perpendicular line L_i (Y_{P_i} axis) to the segment relating P_i and P_{i+1} is imposed to guarantee the navigation liveness (cf. Fig. 3). Once the vehicle oversteps L_i and the vehicle coordinate x^{P_i} in $X_{P_i}Y_{P_i}$ implies that $x^{P_i} \geq 0$, the switch to the next waypoint should take place.

Algorithm 1: Target assignment strategy [42]

Require: Waypoints set, vehicle pose, current target P_i.
Ensure : Sequential switch between waypoints.

if $(d \leq E_d$ ***and*** $e_\theta \leq E_{angle})$ ***or*** $x^{P_i} \geq 0$ **then**
  -Switch to the next waypoint $P_i := P_{i+1}$.
  -Redefine E_d and E_{angle} of the new target.
  -Designate a new local coordinate system $X_{P_i}Y_{P_i}$.
  -Update the vehicle configuration in the new $X_{P_i}Y_{P_i}$.
end

2.3. Safety guarantees for target reaching

An analytical method to define the error maximum thresholds E_d and E_{angle}, while considering the control law parameters, was presented in [42]. It guarantees the control law ability to guide the vehicle to its current target with error values less than or equal to the derived E_d and E_{angle}, while satisfying the vehicle kinematic constraints. The analytical estimation of E_d and E_{angle} given in [42] assumes that the vehicle initial orientation θ_{V_0} to reach the current target is known with a particular range of uncertainty. Nonetheless, the vehicle dynamics and localization while moving towards the target are supposed as precise. This assumption cannot hold true in case of highly uncertain navigation environments. Due to modeling errors, measurement imprecision and several other disturbances, the assumption made in [42] to consider uncertainties can under-estimate risks endangering the NSbSWR. To consider all uncertainties impacting the navigation process while defining E_d and E_{angle}, this paper uses the RA to ensure an appropriate reaching of the target. Compared to the analysis used in [42], a comprehensive online estimation of several modeling/perception uncertainties is included into the NSbSWR framework to ensure the appropriate reaching of waypoints and assess navigation risks.

Aside from the comprehensive estimation of uncertainties to ensure the NSbSWR safety, this work presents another enhancement compared to [42]. Not only the navigation uncertainty-issued threats are captured at an early phase in run-time, but also the control parameters are adapted to overcome these risks (cf. Section 4). Thanks to the adapted controls, the AGV can reach its assigned waypoint while staying always inside the safe/free areas. Together, the RA-based estimation of error boundaries, the analytical relations given in [42] and the proposed strategy to adapt the control parameters build a sound risk management level for the NSbSWR framework.

3. Proposed safety verification/management for NSbSWR

In this paper, a novel safety verification and management level for the NSbSWR is introduced. This latter is constructed through two main steps i.e., the risk assessment and risk management strategies (cf. Fig. 1). To predict potential navigation in forbidden areas (behind the road limits or regions occupied by obstacles), the RA is exploited to perform the risk assessment. Compared to other RA methods (cf. Section 1.2), the Interval Taylor-based RA (ITbRA) provides deterministic results since it does not include any probabilistic prediction. In addition, it uses interval wrappers and does not require any bisection of the system initial states, which offers a valuable simplicity in terms of set-membership calculation and decreases the computational costs [40,46,47]. Notably, the interval-based computation suffers from the pessimism issued from the non-compact form of intervals and the absence of correlation assumptions between the interval variables [37]. In this view, the interval Taylor expansion series are known in the literature as an efficient manner to improve the pessimism [37]. Thus, the ITbRA is selected to perform the risk assessment task for the NSbSWR. Afterwards, a methodological manner to adapt the control parameters and master critical situations is proposed to play as a risk management strategy for the NSbSWR.

3.1. RA-based risk assessment for NSbSWR

In this Subsection, the ITbRA set integration method is detailed. Once a waypoint is assigned, the ITbRA process is triggered to calculate the system reachable sets to appropriately assess the maximum uncertainty that may impact the error between the vehicle and the target poses at the arrival time, while introducing the perception and modeling uncertainties. Hence, the evaluated uncertainties in the final arrival states serve to analysis risks about the ability to reach safely the subsequent waypoints.

3.1.1. ITbRA general scheme

The ITbRA constructs an interval-based model for the studied system while considering uncertainties propagated into its states, initial conditions, controls and parameters. From this scope, the AGV can be described through an uncertain ODE with the following shape:

$$\begin{cases} \dot{x}(t) = f(x, s, p, t) \\ x(t_0) \in [x_0], \quad s \in \mathbb{S}, \quad p \in \mathbb{P} \end{cases} \tag{10}$$

where $f : \mathbb{R}^n \longrightarrow \mathbb{R}^n$ is a non-linear vector-valued function, which defines the system evolution. Accordingly, x is a finite-dimensional state vector of n interval components $[x_{i=1...n}]$. $x(t_0)$ designates the initial domain, which is assigned to the state vector. $\mathbb{S}$ and $\mathbb{P}$ represent respectively the system control sets and the uncertain domain enclosing the ODE parameters.

Let denote the reachable sets of system (10) during an interval time $[t_0, t_f]$ by $\mathscr{R}([t_0, t_f]; [x_0])$. Notably, t_0 is the triggering instant of the RA process. t_f is the satisfaction instant of the waypoint switch conditions (cf. Section 2.2) by the reachable sets (the estimated reachable sets are close enough from the waypoint). Notably, t_f cannot be known posteriorly, but it depends on the vehicle velocity and the number of the integration steps that must be proceeded until reaching the target. Thus, the system forward reachable sets $\mathscr{R}([t_0, t_f]; [x_0])$ between $[t_0, t_f]$ can be formalized via the ODE solutions issued from system (10) with particular initial condition $[x_0]$ as:

$$\mathscr{R}([t_0, t_f]; [x_0]) = \left\{ \begin{matrix} x(\tau), \quad t_0 \leqslant \tau \leqslant t_f \,| \\ (\dot{x}(\tau) = f(x, s, p, \tau)) \wedge (x(t_0) \in [x_0]) \wedge (s \in \mathbb{S}) \wedge (p \in \mathbb{P}) \end{matrix} \right\} \tag{11}$$

Indeed, the form of $\dot{x}(t) = f(x, s, p, t)$ is obtained through a slight modification on the tricycle model given in Eq. (1):

$$\begin{cases} \dot{x}_V(t) = V cos(\theta_V) + w_1 \\ \dot{y}_V(t) = V sin(\theta_V) + w_2 \\ \dot{\theta}_V(t) = V \dfrac{tan(\gamma_V)}{l_b} + w_3 \end{cases} \tag{12}$$

where $(w_1, w_2, w_3)^T$ is the vector of interval-type noises that may affect the process. Bounds of the interval components $w_{i=1..3}$ must enclose all possible states of noises e.g., modeling, perception and measurement errors. At this regard, a prior knowledge of these uncertainties is supposed to be acquired for instance through sensors' features and measurement conditions.

Then, the proposed ITbRA method explores all the possible controls that may be generated within particular uncertain initial states. The min/max bounds of admissible V and γ_V are over-approximated via the interval arithmetic. By dealing with set-valued initial states, the interval arithmetic permits to reveal all the admissible controls at every integration step from $[t_0, t_f]$. The target configuration (x_T, y_T, θ_T) as well as its velocity V_T are assumed as certain. Contrarily, the vehicle pose is henceforth described via interval variables $[x_V], [y_V], [\theta_V]$. Accordingly, $(e_x, e_y, e_\theta, e_{VT}, d)$ can be expressed also through intervals (cf. Section 2.1). Hence, intervals $[V]$ and $[\gamma_V]$ are given by:

$$\begin{cases} [V] = V_T cos([e_\theta]) + [v_b] \\ [\gamma_V] = arctan(l_b[c_c]) \end{cases} \tag{13}$$

Noticeably, $[v_b]$ and $[c_c]$ are calculated in a set-membership manner by substituting $(e_x, e_y, e_\theta, e_{VT}, d)$ by their interval values $([e_x], [e_y], [e_\theta], [e_{VT}], [d])$ in Eqs. (7) and (8). Additionally, l_b (cf. Eq. (1)) is considered as known precisely.

By providing the set-valued controls to the interval Taylor models, $\mathscr{R}([t_0, t_f]; [x_0])$ can be obtained iteratively by finding solutions of system (12) at instants $t_i \in [t_0 \dots t_f]$. Afterwards,

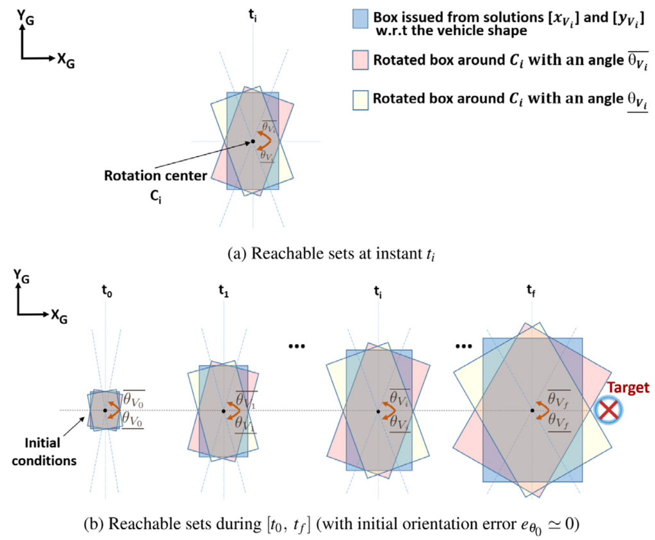

(a) Reachable sets at instant t_i

(b) Reachable sets during $[t_0, t_f]$ (with initial orientation error $e_{\theta_0} \simeq 0$)

Fig. 4. Geometrical representation of reachable sets in the space domain.

solution sets, generated at t_{i-1} starting from $[x_{i-1}]$, are the ODE initial conditions at the next instant t_i. The initial conditions should be updated from iteration to another as follows:

$$\begin{aligned} &[x_1] = f([x_0], s, p, t_0) \\ &[x_2] = f([x_1], s, p, t_1) \\ &\qquad \vdots \\ &[x_i] = f([x_{i-1}], s, p, t_{i-1}) \end{aligned} \tag{14}$$

Evidently, $[V]$ and $[\gamma_V]$ must be recomputed according to new initial conditions at each t_i. The RA process meets its end once bounds of the obtained solution at an instant t_i satisfies the waypoint switch rules (cf. Algorithm 1). Then, the relation $t_f = t_i$ is validated. Suppose that each set solution of Eq. (12) at t_i is denoted $\mathbb{X}_s(t_i)$. Hence, $\mathscr{R}([t_0, t_f]; [x_0])$ is defined as:

$$\mathscr{R}([t_0, t_f]; [x_0]) = \bigcup_{t_i = t_0 \dots t_f} \mathbb{X}_s(t_i) \tag{15}$$

Eq. (15) provides a valuable information support about all the future sets that may be occupied by the vehicle. At each integration step, the solutions of $[x_{V_i}]$ and $[y_{V_i}]$ are represented geometrically in the space domain by an axis-aligned box. This latter must consider also the vehicle geometrical shape (the vehicle length and width). Likewise, the vehicle orientation should also be taken into account. Thus, two simple rotations for the obtained box at t_i are realized, where the point C_i $([mid([x_{V_i}]), \ mid([y_{V_i}])])$ is the rotation center and $\underline{\theta_{V_i}}$ and $\overline{\theta_{V_i}}$ are respectively the performed rotation angles (cf. Fig. 4).

All the vertices of solution boxes of the ODE during $[t_0, \ t_f]$ and those resulting from the rotation are used to bound the vehicle reachable space. A numerically obtained 2D convex hull that encloses all these vertices is used as an envelope of the reachable space. In this sense, Fig. 5 presents an example of boxes enclosing the ODE solutions as well as bounds of the AGV reachable space while moving towards a given assigned target. Finally, the overall RA proposed for NSbSWR is illustrated in the flowchart shown in Fig. 6.

3.1.2. Standard interval Taylor expansion series

As explained, the proposed RA is based on interval Taylor expansion applied during a time grid $t_0 < \cdots < t_i < \cdots < t_f$. In general, Taylor set-integration is initiated by looking for a prior enclosure of the set-solution at an instant t_i. The prior

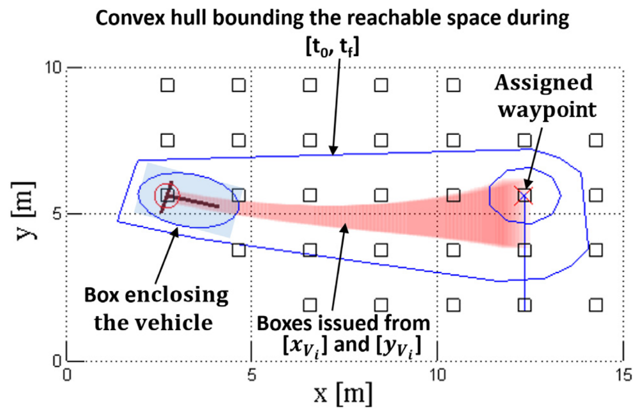

Fig. 5. Reachable space bounding through convex hull enclosure.

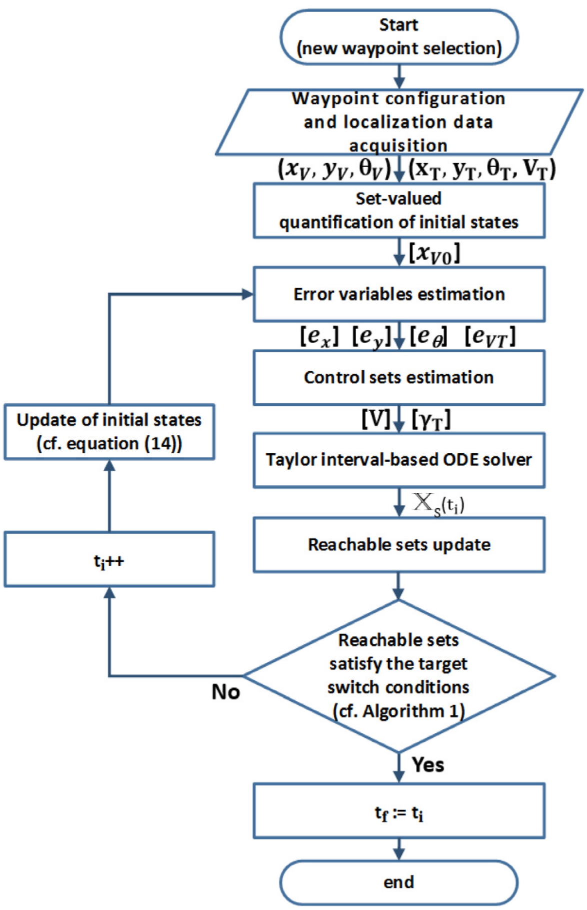

Fig. 6. Flowchart of the proposed RA process for reaching a given waypoint.

guess of regions bounding the solutions are not tight enough [40]. Thus, these regions are further refined to obtain the smallest sets bounding the ODE solutions. In fact, obtaining tight bounds of the vehicle reachable space is essential for the safe reaching of waypoints. Conservative values of E_d and E_{angle} will limit the range of possible choices of the waypoints' locations. To avoid huge error boundary values, the distance between the sequential waypoints would be reduced. Such separation distances between the waypoints may be not sufficient enough to fulfill the asymptotic convergence of the navigation errors to zero. Otherwise, important values of E_d and E_{angle} cannot guarantee that the vehicle is always navigating inside the road limits.

Hence, the prior enclosure of the ODE solution, noted $[\hat{x}_i]$, must satisfy the inclusion test in Eq. (16):

$$\mathbb{X}_s(t) \subset [\hat{x}_i], \quad \forall t \in [t_i, t_{i+1}] \tag{16}$$

During the integration step $\Delta_{t_i} = t_{i+1} - t_i$, the arbitrary guess of $[\hat{x}_i]$ can be realized via the fixed point theorem and the Picard–Lindelö operator [40]. According to these latter, Eq. (17) approximates a first guess of the prior enclosure that satisfies Eq. (16) while minimizing the width of $[\hat{x}_i]$ [40]:

$$[\hat{x}_i] = [x_i] + [0, \Delta_{t_i}]f([x_i], [s], p, [t_i, t_{i+1}]) \tag{17}$$

Then, the prior enclosure is recursively tuned until satisfying:

$$[x_i] + [0, \Delta_{t_i}]f([\hat{x}_i], [s], p, [t_i, t_{i+1}]) \subseteq [\hat{x}_i] \tag{18}$$

Δ_{t_i} can be recursively diminished to satisfy Eq. (18). Rather, $[\hat{x}_i]$ is iteratively enlarged to proceed with an equally spaced time grid and admit an integration step relative to the AGV sampling time. Once the inclusion of Eq. (18) is fulfilled, the recursive estimation of $[\hat{x}_i]$ is stopped. The estimated prior enclosure $[\hat{x}_i]$ is still a conservative approximation of the final solution $[x_{i+1}]$. Thus, the over-approximation of $[x_{i+1}]$ is refined with a Taylor expansion of order k, as shown in Eq. (19). Notably, $[\hat{x}_i]$ is employed to assess the interval remainder r and interval Taylor coefficients $f^{(j)}$:

$$\begin{cases} \mathbb{X}_s(t_i) = [x_{i+1}] = [x_i] + \sum_{j=1}^{k-1} \Delta_{t_i} f^{(j)}([x_i], [s], p, t_i) + r \\ r = \Delta_{t_i} f^{(k)}([\hat{x}_i], [s], p, t_i) \end{cases} \tag{19}$$

where $f^{(j)}$ are interval values obtained numerically or through the successive partial derivatives of f:

$$\begin{aligned} & f^{(0)}([x_i]) = [x_i] \\ & f^{(1)}([x_i]) = f([x_i]) \\ & \quad \vdots \\ & f^{(j)}([x_i]) = \tfrac{1}{j}\left(\tfrac{\partial f^{(j-1)}}{\partial x} f\right)([x_i]) \end{aligned} \tag{20}$$

To recapitulate the earlier discussed steps, the Taylor set-integration method is described in Algorithm 2.

Algorithm 2: Standard interval Taylor method

Inputs : t_i, Δ_{t_i}, and $[x_i]$.
Output: $[x_{i+1}]$.
-Estimate the first guess of $[\hat{x}_i]$ (cf. Eq. (17)).
while $([x_i] + [0, \Delta_{t_i}]f([\hat{x}_i], [s], p, [t_i, t_{i+1}]) \nsubseteq [\hat{x}_i])$ **do**
  -Enlarge the width of $[\hat{x}_i]$.
end
-Calculate interval Taylor coefficients (cf. system (20)).
-Calculate the remainder term r (cf. eq. system (19)).
-Calculate solution $[x_{i+1}]$:
  $[x_{i+1}] = [x_i] + \sum_{j=1}^{k-1} \Delta_{t_i} f^{(j)}([x_i], [s], p, t_i]) + r$

3.1.3. Complexity analysis

The computational cost of a single integration step from the interval Taylor method is $O(k^2)$ [40]. Hence, the overall computational complexity of the interval Taylor expansions applied between the interval time $[t_0, t_f]$ is $O(\alpha k^2)$, where $\alpha = \frac{t_f - t_0}{\Delta_{t_i}}$ is the number of the proceeded integration steps (since a constant time integration step $\Delta_{t_i} = t_{i+1} - t_i$ is used). Besides, a second order expansion ($k = 2$) may be sufficient, since the performed RA methodology takes into account the modeling errors through the intervals noises $(w_1, w_2, w_3)^T$ (cf. eq. system (12)).

Furthermore, an apparent advantage of the flexibility offered by the NSbSWR is removing the complexity problems. As soon

Table 1
Simulation setups for Gaussian uncertainty injection.

Variable	Minimum	Maximum	Mean	Standard deviation
x_v (cm)	−5	5	0	2.5
y_v (cm)	−5	5	0	2.5
θ_v (°)	−0.5	0.5	0	0.25

as a target is assigned via Algorithm 1, the navigation can be carried out with initial values of E_d and E_{angle}. Intuitively, these provisional values are obtained based on the analytical analysis depicted in [42] (by only considering the maximum error of the initial conditions of the vehicle position and orientation). Thus, there is more available time to carry on the RA. Once the reachable space prediction is completed, the temporary fixed E_d and E_{angle} can be updated to take into account the uncertainty propagation into the navigation system.

3.2. ITbRA simulation-based validation work

An extensive simulation work is undertaken to validate the ITbRA under Matlab. The interval computation is proceeded via the INTLAB package [48]. This interval-based computing environment is selected due to its high portability with Matlab, its provable performances, rigorous results and fast computation [48]. Otherwise, the vehicle reachable sets are represented in the 2D space via a computational geometry toolbox.

To prove the ITbRA consistency through quantitative tests, batch simulations are tackled. To be consistent, the ITbRA findings must always include all possible trajectories of the ODE solutions. The reachable space of a given test configuration is calculated. After that, the vehicle real trajectory is estimated until reaching the chosen target while injecting Gaussian noises into the vehicle state (cf. Eq. (12)). It allows to verify whether all the vehicle trajectories issued from executions within Gaussian noises are included into the pre-estimated reachability bounds or not. The magnitude of the injected random noises in each sample time cannot exceed the maximum errors attributed to the interval uncertainties used while proceeding the ITbRA. To deal with the injected stochastic noises during the simulations, an Extended Kalman Filter (EKF) is employed for the AGV localization.

All the simulations presented in this subsection are realized with $V_{max} = 3$ m/s, $\gamma_{V_{max}} = 20°$ and $V_T = 1$ m/s. Among numerous realized batch simulations, let us consider a given test scenario where Gaussian uncertainties are injected in the navigation dynamics according to the setups shown in Table 1. To estimate the system reachable space within same minimum/maximum values of stochastic uncertainties, bounds of the interval noises attributed to (x_V, y_V, θ_V) at every sample time are respectively ±5 cm, ±5 cm and ±0.5°.

Including 200 triggered execution, the batch simulation results in the 2-dimensional space are presented in Fig. 7. Afterwards, the evolution of (x_V, y_V, θ_V) obtained via batch simulations and their corresponding reachability-issued frames are illustrated in Figs. 8–10.

The depicted results prove that the ITbRA-issued bounds enclose perfectly the data obtained via the batch simulations and a successful estimation of the reachable space was undertaken. Thus, the ITbRA reliability in ensuring safety verification for the NSbSWR framework is proved.

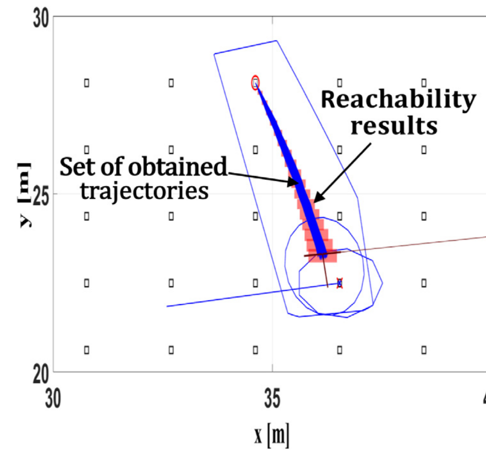

Fig. 7. Batch simulation results representation in 2D space.

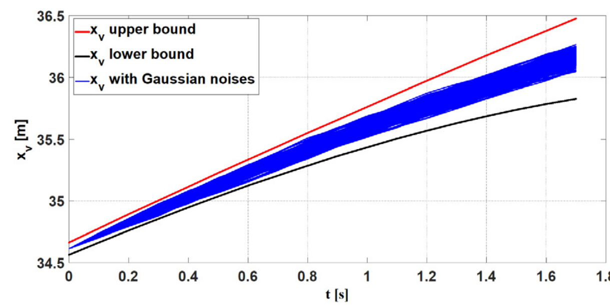

Fig. 8. Evolution of x_V compared to reachable space bounds.

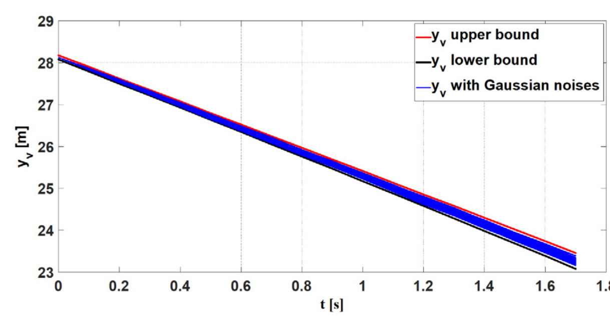

Fig. 9. Evolution of y_V compared to reachable space bounds.

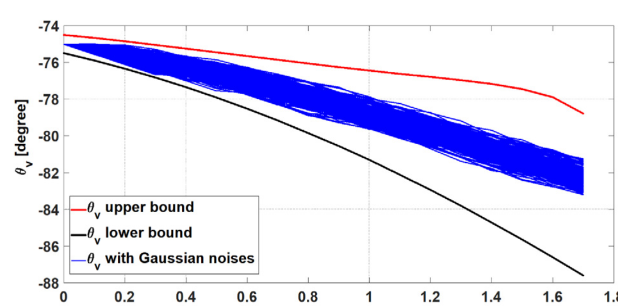

Fig. 10. Evolution of θ_V compared to reachable space bounds.

4. ITbRA-based risk management for NSbSWR

Typically, the use of the RA approaches in the literature is restricted to perform the in-road risk assessment. At the best of our knowledge, this is the first work that establishes a strong link between RA and the control layer to master the predicted risks. The ITbRA outputs are exploited in the sequel to maintain a predefined Lower Distance (LD) to the road limit (or obstacles for certain contexts) as shown in Fig. 11.

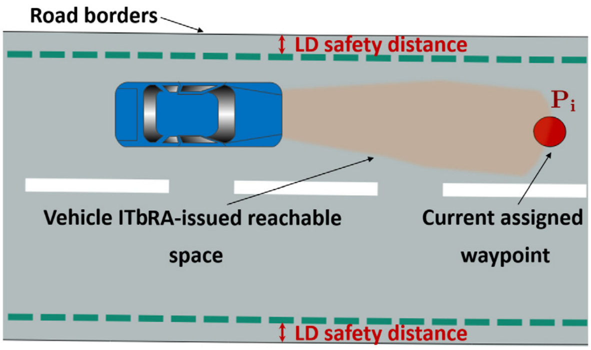

Fig. 11. ITbRA-based risk management principle.

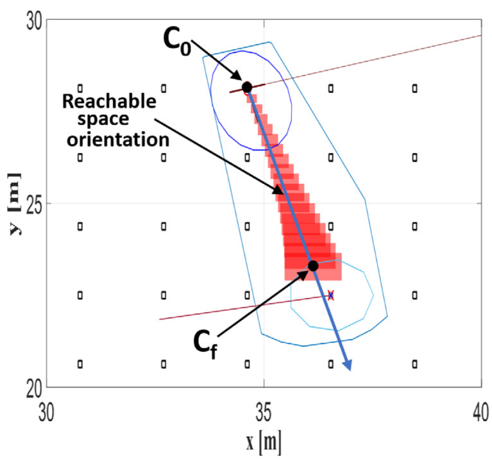

Fig. 12. Orientation of the bounded reachable space.

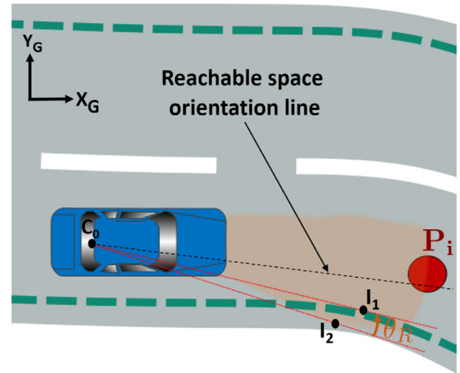

Fig. 13. θ_R estimation method.

4.1. Proposed risk management algorithm for NSbSWR

As stated earlier, the control stability is guaranteed for all positive parameters (K_d, K_l, K_o, K_x, K_{VT}, K_θ) [42]. In particular, K_θ is the parameter influencing on the vehicle angular velocity. Notably, e_θ is assumed to converge asymptotically towards zero. Through this assumption, Eqs. (6) and (8) imply:

- For $e_\theta \in]0, \pi/2[$, the term $k_\theta\ tan(e_\theta)$ in Eq. (8) is positive. Hence, rising k_θ will deviate the reachable space orientation to the anticlockwise direction (since $\gamma_V = \arctan(l_b c_c) \longrightarrow \pi/2$). Contrarily, if k_θ drops to zero then the orientation of the vehicle reachable space will move towards the clockwise direction.
- For $e_\theta \in]-\pi/2, 0[$ and based on the sign of $k_\theta\ tan(e_\theta)$, increasing/decreasing the value of k_θ will entail respectively the re-orientation of the vehicle reachable space to the clockwise/anticlockwise direction.

Accordingly, the orientation of the AGV reachable space can be changed to always stay in the safe/free areas. The line linking the center of the initial condition box C_0 and the center C_f of the reached box at t_f is assumed to outline approximately the direction of the reachable space (cf. Fig. 12). As soon as an intersection between reachable state space and forbidden regions is predicted, a new value of K_θ is selected to guide the AGV to safe zones. Generally, the navigation should be proceeded with the nominal value chosen for K_θ. At instant t_f, intersections between the road limits and the AGV reachable space should be verified. If no intersection is found, the nominal value of K_θ is kept. In the other case, K_θ is updated until reaching the current assigned waypoint without crossing the forbidden zone. The new K_θ value aims to rotate the reachable space shape around the center C_0 of the initial condition domain with an angle θ_R to prevent any intersection between the reachable state space and forbidden regions. θ_R is determined via the angle between the following lines (cf. Fig. 13):

- The line crossing C_0 and I_1, which is the closest point from the road boundary (in intersection with the system reachable space) to the convex shape orientation line.
- The line crossing C_0 and the point I_2. This latter is the most distant point belonging to the convex hull bound (located behind the road margins) from the road segment in intersection with the road borders.

In practice, the road boundaries may be considered as a polyline relating points from the borders. Hence, I_1 and I_2 can be determined via several computational geometry algorithms. The proposed risk management solution can be easily applied to avoid obstacles in the AGV pathway (cf. Section 4.2).

In this work, consequences of adapting the nominal value of K_θ on the reachable space orientation are determined by offline simulations. While using extensive offline tests with large equally spaced values of K_θ, the different changes in the reachable space orientation are stored. According to these results, the most suitable new K_θ is picked up to achieve the required θ_R. The proposed risk management strategy for the safe reaching of waypoints under uncertainty is summarized in Algorithm 3.

4.2. Simulation results

To prove the efficiency of Algorithm 3, a NSbSWR simulation scenario to cross two sharp road bends is tackled under Matlab. As shown in Fig. 14, the risk of crossing the first road deviation is increased by the presence of another vehicle (a static obstacle). The borders represented in gray in Fig. 14 are the concrete road limits. The borders drawn in green are the road boundaries after setting a safety distance LD = 1 m. The vehicle initial pose is: $x_V = 7.8$ m, $y_V = 16.9$ m and $\theta_V = -70°$. A set of twelve waypoints are designated to guide the vehicle. The waypoints' locations are selected in many occasions close to the road borders to invoke critical situations (cf. Table 2). Otherwise, every waypoint's configuration is joined with specific error values to define its own error circle.

At first, the simulation is executed without applying Algorithm 3. The nominal control parameters are maintained all along the navigation run-time, where $K_d = 0.1$, $K_l = 1.8$, $K_o = 60$, $K_x = 0.4$, $K_{VT} = 0.01$ and $K_\theta = 0.19$. The navigation is proceeded with a maximum velocity $V_{max} = 10$ m/s, a maximum front wheel

Table 2
Waypoints configurations.

	P_1	P_2	P_3	P_4	P_5	P_6	P_7	P_8	P_9	P_{10}	P_{11}	P_{12}
x_T (m)	9.6	13.5	19.2	23	27	30.8	32.7	34.6	36.5	40.4	42.3	44.2
y_T (m)	11.3	5.6	5.6	5.6	11.3	16.9	20.6	22.5	22.5	18.8	13.1	5.6
$\theta_T(°)$	−55.6	0	0	55.6	55.6	62.9	44.3	0	−44.3	−71.1	−75.6	−90

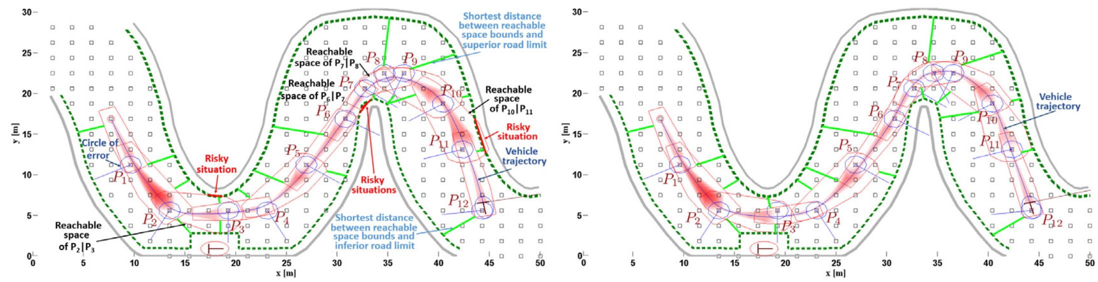

(a) NSbSWR simulation results within nominal control parameters

(b) NSbSWR simulation results within ITbRA-based risk management

Fig. 14. Simulations without/without adaptive gain control (available at: https://bit.ly/2TjP9Gp). (For interpretation of the references to color in this figure legend, the reader is referred to the web version of this article.)

Algorithm 3: ITbRA-based risk management strategy

Require: Waypoints set, vehicle pose, current target P_i.
Ensure : Safety guarantees for the NSbSWR.

```
while NSbSWR process is running do
    if new waypoint is assigned then
        -Proceed ITbRA within nominal kθ.
        -Check collision risks.
        if no collisions are observed then
            repeat
                -Proceed navigation with nominal kθ.
            until reaching the assigned waypoint
        else
            repeat
                -Estimate θR.
                -Adapt kθ based on the offline results.
            until reaching the assigned waypoint
        end
        -Switch to new waypoint Pi := Pi+1.
    end
end
```

Table 3
Interval-type uncertainty injection setups.

Uncertainty bounds	Periods
(±10 cm, ±10 cm, ±0.5°)	$P_3\|P_4$, $P_5\|P_6$, $P_6\|P_7$, $P_7\|P_8$, $P_8\|P_9$
(±10 cm, ±10 cm, ±1°)	$P_2\|P_3$
(±15 cm, ±15 cm, ±0.5°)	$P_4\|P_5$, $P_{11}\|P_{12}$
(±15 cm, ±15 cm, ±0.8°)	$P_0\|P_1$, $P_9\|P_{10}$
(±15 cm, ±15 cm, ±1°)	$P_1\|P_2$, $P_{10}\|P_{11}$

orientation $\gamma_{V_{max}} = 20°$, and a sampling step equal to 0.02 *s*. All the waypoints' velocities are set to $V_T = 5$ m/s.

Let denote by $P_i|P_{i+1}$ the period when the vehicle is traveling from the waypoint P_i until reaching P_{i+1}. $P_0|P_1$ refers to the travel time between the vehicle initial position and waypoint P_1. The extent of interval-type uncertainties injected into the NSbSWR framework to conduct the ITbRA during all periods $P_i|P_{i+1}$ are detailed in Table 3. Remarkably, these extents are attributed to the system initial conditions and noises (w_1, w_2, w_3) (cf. Eq. (12)). Besides, white noises are injected into the navigation system variables to estimate its real trajectory.

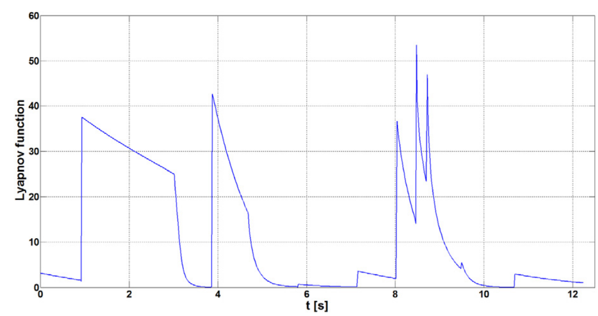

Fig. 15. Lyapunov function of adopted control law.

Fig. 14a illustrates the overall results of this first simulation scenario in the 2D space domain. The thick green segments in Fig. 14a represent the shortest distance separating bounds of the navigation system reachable space and the road boundaries from both sides. These segments approve the safety of the navigation towards the next waypoint. In contrast, the red thick segments underline the regions in intersection with the road safety margins. Accordingly, four potential collisions between the vehicle and the road borders are captured during the simulation runtime. Actually, these collisions are detected respectively during periods $P_2|P_3$, $P_6|P_7$, $P_7|P_8$ and $P_{10}|P_{11}$.

The controller stability is analyzed via the Lyapunov function V_L (cf. Eq. (3)). According to Fig. 15, the generated controls are able to ensure the asymptotic stability and the convergence to every waypoint.

Otherwise, Fig. 16 exhibits the evolution of the navigation errors in terms of distance to the target and the difference in orientation between the target and vehicle. Accordingly, the proposed control decreases steadily the mentioned errors. Noticeably, the distance to target never reaches zero since the switch between the waypoints is triggered once the vehicle crosses the error circle of a given target.

Then, a second simulation scenario is realized to test the introduced risk management in terms of safety assurance. As shown in Fig. 14b, all the collision risks are handled through Algorithm 3. The nominal value of K_θ was tuned in three occasions (periods $P_2|P_3$, $P_6|P_7$ and $P_{10}|P_{11}$). The earlier captured collision in period $P_7|P_8$ was systematically mastered since the vehicle changed its trajectory during period $P_6|P_7$. Table 4 reveals the applied modification in K_θ based on the offline results.

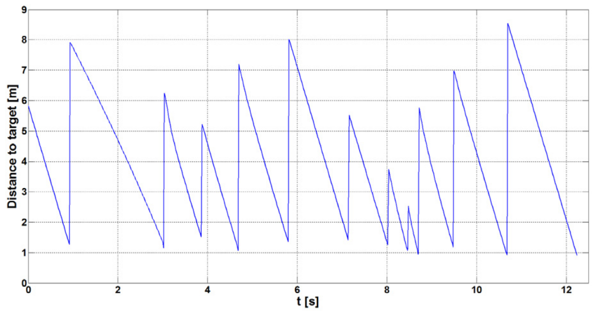

(a) Evolution of distance to current assigned target

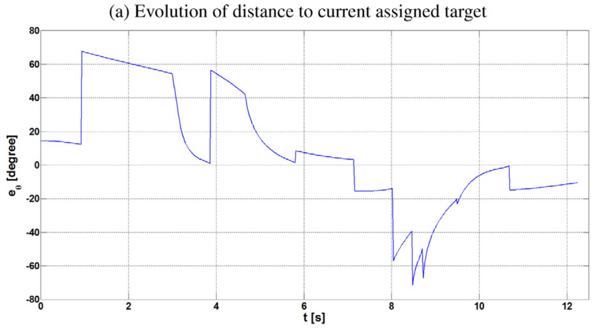

(b) Evolution of angular orientation error

Fig. 16. Distance/angular errors with nominal control parameters.

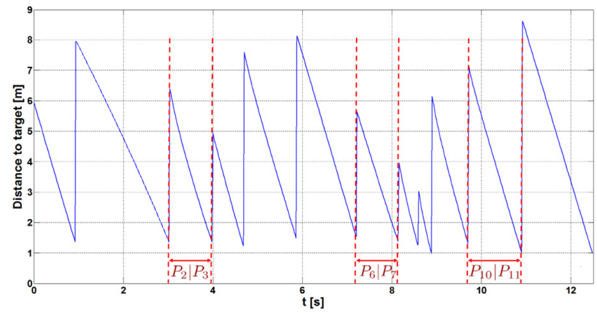

(a) Evolution of distance to current assigned target

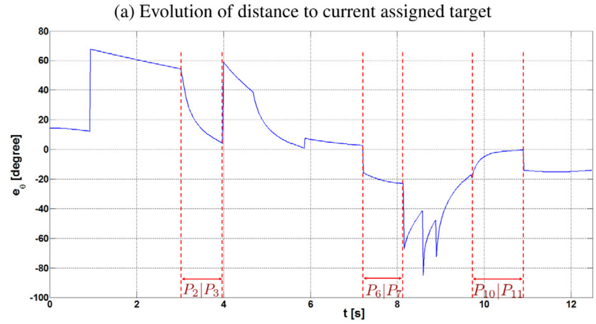

(b) Evolution of angular orientation error

Fig. 18. Distance/angular errors with adapted control parameters.

Table 4
Risk management modifications in control parameters.

Period	$P_2\|P_3$	$P_6\|P_7$	$P_{10}\|P_{11}$
θ_R (°)	3.3°	8.3°	3.9°
Direction	Clockwise	Anti-clockwise	Clockwise
Adapted K_θ	0.143	0.07	0.263

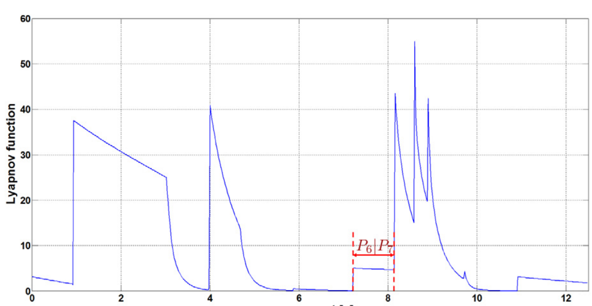

Fig. 17. Lyapunov function after adapting the control parameters.

The results in Fig. 17 confirms the navigation asymptotic stability even within the modification in K_θ. The same shape of the Lyapunov function is obtained compared to the results in Fig. 15. Remarkably, the fall in the Lyapunov function during period $P_6|P_7$ ($[7.22s, 8.14s]$) is less important. Indeed, this period witnessed the most important change in K_θ to enable the required re-orientation angle θ_R. Despite of this change in the Lyapunov function, the NSbSWR stability is still maintained.

Finally, Fig. 18 shows the evolution of navigation errors (distance and orientation w.r.t the target). Compared to the first simulation scenario, the performed changes in k_θ invoked a slight decrease in the convergence rate of e_θ during $P_2|P_3$ and $P_{10}|P_{11}$. The impacts of the applied modifications on the orientation error e_θ is more obvious during $P_6|P_7$. Otherwise, the error in terms of final distance to the target is more important than the nominal case during $P_6|P_7$ and $P_{10}|P_{11}$. The realized validation work demonstrated the proposed risk management efficiency. The adopted Lyapunov-based control law maintains always the navigation stability regardless to the value of k_θ (which must be positive). Safety is guaranteed for the NSbSWR with a harmless loss of precision in the convergence of the navigation system to its target even in worst uncertain case.

5. Conclusion

Due to its high flexibility, more attention is paid recently to the Navigation Strategy based on Sequential Waypoint Reaching (NSbSWR) strategies to avoid several trajectory planning/re-planing complex tasks. In this paper, the interval analysis is used to provide online safety guarantees for a particular NSbSWR strategy. The introduced risk management allows to consider several uncertainties as modeling and perception errors. An uncertain ODE, which describes the navigation according to NSbSWR, is resolved via the interval Taylor method. All potential reachable sets of the navigation future states are revealed. More over, an important link between the control layer and the study of reachability space is established to satisfy the safety requirements. It provides efficient feedback solutions for the NSbSWR once a collision is predicted. Safety is ensured by adapting the control parameters to influence the location of the most probable reachable space and guarantee thus non collision of the vehicle with the forbidden area. The ability of the proposed RA to enclose all possible future states of the navigation under uncertainty is demonstrated via extensive batch simulations. Even more, a convenient simulation scenario was established to test the suggested re-configuration of the adopted controller based on reachability. The simulation results showed that the collision risks have been mastered under uncertainty.

The reachability results should be exploited to define optimal and safe configurations of waypoints in the future. More efficient adaptive control parameters technique should be studied to guarantee a better and faster re-shaping of the vehicle reachable space. Finally, the required technical steps to succeed the implementation of the proposed reachability solution into a real vehicle will be addressed in another future work.

Declaration of competing interest

The authors declare that they have no known competing financial interests or personal relationships that could have appeared to influence the work reported in this paper.

Acknowledgment

This work received the support of IMobS3 Laboratory of Excellence (ANR-10-LABX-16-01). This work also received the support of the Hauts-de-France CPER (Contrats de Plan État-Région), through the RITMEA (Recherche et Innovation en Transports et Mobilités Eco-responsables et Automatisées) project.

References

[1] W. Lim, S. Lee, M. Sunwoo, K. Jo, Hybrid trajectory planning for autonomous driving in on-road dynamic scenarios, IEEE Trans. Intell. Transp. Syst. 22 (1) (2021) 341–355.
[2] O. Sharma, N. Sahoo, N. Puhan, Recent advances in motion and behavior planning techniques for software architecture of autonomous vehicles: A state-of-the-art survey, Eng. Appl. Artif. Intell. 101 (2021) 104211.
[3] Y. Brouwer, A. Vale, R. Ventura, Informative path planner with exploration–exploitation trade-off for radiological surveys in non-convex scenarios, Robot. Auton. Syst. 136 (2021) 103691.
[4] L. Adouane, Reactive versus cognitive vehicle navigation based on optimal local and global pelc*, Robot. Auton. Syst. 88 (2017) 51–70.
[5] X. Di, R. Shi, A survey on autonomous vehicle control in the era of mixed-autonomy: From physics-based to AI-guided driving policy learning, Transp. Res. C 125 (2021) 103008.
[6] M.W. Mehrez, K. Worthmann, J.P. Cenerini, M. Osman, W.W. Melek, S. Jeon, Model predictive control without terminal constraints or costs for holonomic mobile robots, Robot. Auton. Syst. 127 (2020) 103468.
[7] Q. Chen, Y. Xie, S. Guo, J. Bai, Q. Shu, Sensing system of environmental perception technologies for driverless vehicle: A review of state of the art and challenges, Sensors Actuators A 319 (2021) 112566.
[8] N.M.B. Lakhal, O. Nasri, L. Adouane, J.B.H. Slama, Controller area network reliability: overview of design challenges and safety related perspectives of future transportation systems, IET Intell. Transp. Syst. 14 (2020) 1727–1739.
[9] M. Martínez-Díaz, F. Soriguera, Autonomous vehicles: theoretical and practical challenges, Transp. Res. Proc. 33 (2018) 275–282, XIII Conference on Transport Engineering, CIT2018.
[10] B. Li, Y. Zhang, Y. Feng, Y. Zhang, Y. Ge, Z. Shao, Balancing computation speed and quality: A decentralized motion planning method for cooperative lane changes of connected and automated vehicles, IEEE Trans. Intell. Veh. 3 (3) (2018) 340–350.
[11] J. Vilca, L. Adouane, Y. Mezouar, Optimal multi-criteria waypoint selection for autonomous vehicle navigation in structured environment, J. Intell. Robot. Syst. 82 (2) (2016) 301–324.
[12] N. Wang, H.R. Karimi, Successive waypoints tracking of an underactuated surface vehicle, IEEE Trans. Ind. Inf. 16 (2) (2020) 898–908.
[13] A.A. Masoud, A harmonic potential approach for simultaneous planning and control of a generic UAV platform, J. Intell. Robot. Syst. 65 (1) (2012) 153–173.
[14] Y. Wang, D. Mulvaney, I. Sillitoe, E. Swere, Robot navigation by waypoints, J. Intell. Robot. Syst. 52 (2) (2008) 175–207.
[15] D.C. Rao, M.R. Kabat, P.K. Das, P.K. Jena, Hybrid IWD-DE: A novel approach to model cooperative navigation planning for multi-robot in unknown dynamic environment, J. Bionic Eng. 16 (2) (2019) 235–252.
[16] D. Herrero, J. Villagrá, H. Martínez, Self-configuration of waypoints for docking maneuvers of flexible automated guided vehicles, IEEE Trans. Autom. Sci. Eng. 10 (2) (2013) 470–475.
[17] C. Sprunk, B. Lau, P. Pfaff, W. Burgard, An accurate and efficient navigation system for omnidirectional robots in industrial environments, Auton. Robots 41 (2) (2017) 473–493.
[18] H. Cheon, B.K. Kim, Online bidirectional trajectory planning for mobile robots in state-time space, IEEE Trans. Ind. Electron. 66 (6) (2019) 4555–4565.
[19] W. Gu, S. Cai, Y. Hu, H. Zhang, H. Chen, Trajectory planning and tracking control of a ground mobile robot:A reconstruction approach towards space vehicle, ISA Trans. 87 (2019) 116–128.
[20] P. Nowak, T.C. Stewart, A spiking model of desert ant navigation along a habitual route, in: R. Matoušek (Ed.), Recent Advances in Soft Computing, Springer International Publishing, Cham, 2019, pp. 211–222.
[21] J.-S. Yoon, B.-C. Min, S.-O. Shin, W.-S. Jo, D.-H. Kim, Ga-based optimal waypoint design for improved path following of mobile robot, in: J.-H. Kim, E.T.. Matson, H. Myung, P. Xu, F. Karray (Eds.), Robot Intelligence Technology and Applications 2: Results from the 2nd International Conference on Robot Intelligence Technology and Applications, Springer International Publishing, Cham, 2014, pp. 127–136.
[22] D.M. Lyons, R.C. Arkin, S. Jiang, T. Liu, P. Nirmal, Performance verification for behavior-based robot missions, IEEE Trans. Robot. 31 (3) (2015) 619–636.
[23] M. Althoff, J.M. Dolan, Online verification of automated road vehicles using reachability analysis, IEEE Trans. Robot. 30 (4) (2014) 903–918.
[24] H. Guéguen, M.-A. Lefebvre, J. Zaytoon, O. Nasri, Safety verification and reachability analysis for hybrid systems, Annu. Rev. Control 33 (1) (2009) 25–36.
[25] S. Manzinger, C. Pek, M. Althoff, Using reachable sets for trajectory planning of automated vehicles, IEEE Trans. Intell. Veh. (2020) 1.
[26] T. Brudigam, M. Olbrich, D. Wollherr, M. Leibold, Stochastic model predictive control with a safety guarantee for automated driving, IEEE Trans. Intell. Veh. (2021) 1.
[27] M. Althoff, A. Mergel, Comparison of Markov chain abstraction and Monte Carlo simulation for the safety assessment of autonomous cars, IEEE Trans. Intell. Transp. Syst. 12 (4) (2011) 1237–1247.
[28] J. Suh, H. Chae, K. Yi, Stochastic model-predictive control for lane change decision of automated driving vehicles, IEEE Trans. Veh. Technol. 67 (6) (2018) 4771–4782.
[29] N. Malone, H. Chiang, K. Lesser, M. Oishi, L. Tapia, Hybrid dynamic moving obstacle avoidance using a stochastic reachable set-based potential field, IEEE Trans. Robot. 33 (5) (2017) 1124–1138.
[30] J. Nicola, L. Jaulin, Comparison of Kalman and interval approaches for the simultaneous localization and mapping of an underwater vehicle, in: L. Jaulin, A. Caiti, M. Carreras, V. Creuze, F. Plumet, B. Zerr, A. Billon-Coat (Eds.), Marine Robotics and Applications, Springer International Publishing, Cham, 2018, pp. 117–136.
[31] L. Schafer, S. Manzinger, M. Althoff, Computation of solution spaces for optimization-based trajectory planning, IEEE Trans. Intell. Veh. (2021) 1.
[32] K. Driggs-Campbell, V. Govindarajan, R. Bajcsy, Integrating intuitive driver models in autonomous planning for interactive maneuvers, IEEE Trans. Intell. Transp. Syst. 18 (12) (2017) 3461–3472.
[33] N.M.B. Lakhal, L. Adouane, O. Nasri, J.B.H. Slama, Interval-based solutions for reliable and safe navigation of intelligent autonomous vehicles, in: 2019 12th International Workshop on Robot Motion and Control (RoMoCo), Poznań, Poland, 2019, pp. 124–130.
[34] M. Maïga, N. Ramdani, L. Travé-Massuyès, C. Combastel, A comprehensive method for reachability analysis of uncertain nonlinear hybrid systems, IEEE Trans. Automat. Control 61 (9) (2016) 2341–2356.
[35] H.N.V. Pico, D.C. Aliprantis, Reachability analysis of linear dynamic systems with constant, arbitrary, and Lipschitz continuous inputs, Automatica 95 (2018) 293–305.
[36] T. Nguyen, T. Au, A constant-time algorithm for checking reachability of arrival times and arrival velocities of autonomous vehicles, in: 2019 IEEE Intelligent Vehicles Symposium (IV), 2019, pp. 2039–2044.
[37] L. Jaulin, M. Kieffer, O. Didrit, E. Walter, Applied Interval Analysis with Examples in Parameter and State Estimation, Robust Control and Robotics, Springer, London, 2001.
[38] S. Rohou, L. Jaulin, L. Mihaylova, F.L. Bars, S.M. Veres, Guaranteed computation of robot trajectories, Robot. Auton. Syst. 93 (2017) 76–84.
[39] R.E. Moore, Interval analysis: differential equationsinterval analysis: Differential equations, in: C.A. Floudas, P.M. Pardalos (Eds.), Encyclopedia of Optimization, Springer US, Boston, MA, 2009, pp. 1685–1689.
[40] N. Ramdani, N. Meslem, Y. Candau, A hybrid bounding method for computing an over-approximation for the reachable set of uncertain nonlinear systems, IEEE Trans. Automat. Control 54 (10) (2009) 2352–2364.
[41] X. Liao, K. Liu, H. Niu, J. Luo, Y. Li, L. Qin, An interval taylor-based method for transient stability assessment of power systems with uncertainties, Int. J. Electr. Power Energy Syst. 98 (2018) 108–117.
[42] J. Vilca, L. Adouane, Y. Mezouar, A novel safe and flexible control strategy based on target reaching for the navigation of urban vehicles, Robot. Auton. Syst. 70 (2015) 215–226.
[43] J.-M. Vilca, L. Adouane, Y. Mezouar, Reactive navigation of mobile robot using elliptic trajectories andeffective on-line obstacle detection, Gyrosc. Navig. J. 4 (1) (2013) 14–25, Ed. Springer, Russia, ISSN 2075 1087.
[44] N.M.B. Lakhal, L. Adouane, O. Nasri, J.B.H. Slama, Risk management for intelligent vehicles based on interval analysis of ttc, IFAC-PapersOnLine 52 (8) (2019) 338–343, 10th IFAC Symposium on Intelligent Autonomous Vehicles IAV 2019.
[45] J. Vilca, L. Adouane, Y. Mezouar, Stable and flexible multi-vehicle navigation based on dynamic inter-target distance matrix, IEEE Trans. Intell. Transp. Syst. 20 (4) (2019) 1416–1431.

[46] H. Dbouk, S. Schön, Comparison of different bounding methods for providing gps integrity information, in: IEEE/ION Position, Location and Navigation Symposium (PLANS), 2018, pp. 355–366, Monterey, USA.
[47] X. Yang, J.K. Scott, Efficient reachability bounds for discrete-time nonlinear systems by extending the continuous-time theory of differential inequalities, in: Annual American Control Conference, 2018, pp. 6242–6247.
[48] S. Rump, INTLAB - INTerval LABoraTory, in: T. Csendes (Ed.), Developments in Reliable Computing, Kluwer Academic Publishers, Dordrecht, 1999, pp. 77–104.

Nadhir Mansour Ben Lakhal is carrying his research work in robotics and automatic control. His Ph.D is a joint program between Clermont Auvergne University (France) and University of Sousse (Tuinisia). He received his engineering degree in Industrial Electronics in 2014 and his Master's degree in Intelligent and Communicating Systems in 2015 from the National Engineering School of Sousse, Tunisia. He focalizes his research on vehicle/robot safe autonomous navigation and risk management development for intelligent vehicles.

Lounis Adouane is a full Professor at Université de Technologie de Compiègne (UTC, France). He received the Ph.D. degree in automatic control from the FEMTO-ST Laboratory, ENSMM, in 2005. During his Ph.D. studies, he deeply investigated the field of mobile multi-robot systems; especially those related to bottom-up and decentralized control architectures. In 2005, he joined the Ampere Laboratory, INSA Lyon, and he studied hybrid (continuous/discrete) control architectures applied to cooperative mobile robots arms. In 2015, he obtained an HDR (habilitation to steer research in robotics) from Blaise Pascal University. From 2006 to 2019, he was an Associate Professor at the Institut Pascal, Polytech Clermont-Ferrand. Currently, Lounis Adouane holds a full Professor position at Heudiasyc, UMR 7253 CNRS/UTC. Between 2018 and 2019, he was the head of ISPR Group (Images, Perception Systems and Robotics, 80 members) at Institut Pascal. Since 2018, Prof. Lounis Adouane is a member of the Technical Committee of IFAC–Intelligent Autonomous Vehicles and serves in the Editorial Board of the Journal of Intelligent and Robotic Systems. Prof. Lounis Adouane is the author/coauthor of more than 120 refereed international papers and two books. His main research interest includes planning and control of mobile robots/intelligent vehicles (autonomous and clean), decision-making under uncertainty, hybrid (continuous/discrete) and hybrid (reactive/cognitive) multi-controller architectures, Lyapunov-based synthesis and stability, cooperative multi-robot systems, artificial intelligence (e.g., MDP or MAS approaches), energy management (e.g., optimal control or neuro-fuzzy approaches).

Othman Nasri received the M.S Degree in Control Systems and Applied Informatics from Ecole Centrale de Nantes, France, in 2004, and the Ph.D. degree in automatic control, with emphasis on the safety verification for hybrid systems from Centrale Supelec university of Rennes-France, in 2007. From 2008 to 2010, he was a researcher Engineer in Embedded Control Systems in University of Paris-Sud 11/ INRIA Saclay Île-De-France. He joined the National Engineering School of Sousse and the Laboratory of Advanced Technology and Intelligent Systems, University of Sousse, Tunisia, in 2010. In 2019, he received the Habilitation in electrical engineering from University of Sousse, Tunisia, with emphasis on the supervision and diagnosis of industrial systems. His current research interests revolve around Fault Detection, Isolation and Recovery (FDIR) techniques, with application to smart systems and autonomous robotics in presence of uncertainty and/or faults. He works mainly on interval observers, multivariate statistical approaches, risk management for autonomous navigation and reachability analysis.

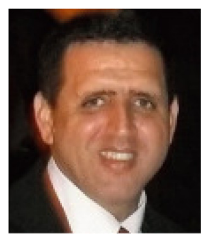

Jaleleddine Ben Hadj Slama (SM'13) received the engineer and the Ph.D. degrees, both in Electrical Engineering, from Ecole Centrale de Lyon, Lyon, France, in July 1994 and December 1997 respectively. Since 2015, he is full Professor in Electrical Engineering at the National Engineering School of Sousse, Tunisia, where he is the leader of the power quality research group in the LATIS laboratory, his main research interests include reliability of transportation systems, Electromagnetic Compatibility (EMC), near-field techniques, EMI issues of power electronics systems and their modeling, Smart Grid, Green datacenters, Renewable Energy and development of remote laboratories for Internet Based Engineering Education.